NANO LETTERS

2003
Vol. 3, No. 2
261−264

Platinum-Maghemite Core–Shell Nanoparticles Using a Sequential Synthesis

Xiaowei Teng,[†] Donald Black,[||] Neil J. Watkins,[‡] Yongli Gao,[‡] and Hong Yang*[,†,§]

Department of Chemical Engineering and Physics and Astronomy and Laboratory for Laser Energetics, University of Rochester, Rochester, New York 14627, and Imaging Materials & Media, R&D, Eastman Kodak Company, Rochester, New York 14650

Received November 26, 2002; Revised Manuscript Received December 13, 2002

ABSTRACT

Pt@Fe_2O_3 core–shell nanoparticles have been made using a sequential synthetic method. Platinum nanoparticles were synthesized via reduction of platinum acetylacetonate in octyl ether, and layers of iron oxide were subsequently deposited on the surface of Pt nanoparticles through thermal decomposition of iron pentacarbonyl. The core–shell nanoparticles were characterized by powder X-ray diffraction, high-resolution transmission electron microscopy, and X-ray photoemission spectroscopy. Thickness of the shell can be controlled by changing concentrations of the reactants and the reaction conditions. These Pt@Fe_2O_3 core–shell nanoparticles could have potential applications in catalysis and as precursors for making property-tunable magnetic nanoparticles, thin films, and nanocomposites.

We present in this letter a one-pot sequential synthetic method of well-defined and shell-thickness-tunable Pt@Fe_2O_3 core−shell nanoparticles. Transition metal containing nanoparticles have been under investigation for quite some time because of their catalytical, electronic, magnetic, and optical properties, and the new applications in various emerging fields such as ultrahigh-density magnetic storage media, biological labeling and detection, and drug delivery.[1−13] Among various systems, transition metal containing core−shell nanoparticles are particularly interesting because these systems can have multiple functions that do not exist in single-component compounds and unique properties that exist only in nm-sized materials. For instance, core−shell nanoparticles have been tested as catalysts in various chemical reactions, and both core and shell are actively involved in the catalytic processes.[5,6,14,15] Klabunde and co-workers have demonstrated that Fe_2O_3-coated metal oxide core−shell nanoparticles such as Fe_2O_3@MgO and Fe_2O_3@CaO have greatly enhanced efficiencies over pure MgO and CaO catalysts for SO_2 adsorption, H_2S removal, and chlorocarbon destruction.[16−18] This uncommon catalytic behavior comes from the cooperative interaction between reactants and both the cores and the shells of the catalysts. Recently, Luo and others have shown that gold-based core−shell nanoparticles can catalyze electrooxidation of methanol.[14,19] Metal-oxide-on-metal core−shell configuration (Au@AuO_x) is believed to be the contributing factor for the high catalytic behaviors. Chen and co-workers show that well-balanced bimetallic surfaces of nickel on platinum can drastically enhance the catalytic hydrodesulfurization (HDS) of thiophene per surface metal atom over pure platinum surface.[20] Such enhancement preferably exists on surfaces with a single layer of nickel on platinum. It is, therefore, very important to develop new methods that can be used to synergistically control chemical compositions, monodispersity, and hierarchical structure of nanoparticles.

Steady progress has been made in recent years in the fine control of chemical composition, structure and monodispersity of inorganic core−shell nanoparticles in solution phases.[2,21−37] These core−shell nanoparticles were generally synthesized through two major synthetic pathways: precipitation and surface reaction and controlled deposition using preformed primary particles.[2] The latter method is generally used for making relatively large-sized core−shell particles, and fine control can be achieved through layer-by-layer (LbL) depositions. The former approach has been extensively used in the synthesis of nm-sized core−shell particles. Silica, titania, and other oxide shells derived from alkoxide reactants are the most common materials, and the corresponding sol−gel processes including the Stöber method have been extensively applied.[23−26] In these systems, reaction conditions generally need to be optimized to minimize shell irregularity and particle aggregation.[2]

* Corresponding author. E-mail: hongyang@che.rochester.edu; Telephone: (585) 275-2110; Fax: (585) 273-1348.
[†] Department of Chemical Engineering.
[‡] Department of Physics and Astronomy.
[§] Laboratory for Laser Energetics.
[||] Imaging Materials & Media.

10.1021/nl025918y CCC: $25.00
Published on Web 01/11/2003

We choose to study Fe−Pt based nanoparticles partially because of the recent success in making monodisperse FePt alloy nanoparticles using polyol process.[4,8,38,39] The straightforward control of $Fe(CO)_5$ deposition is also a valuable feature. We were motivated by the existing and potential applications of Fe and Pt-containing nanoparticles as well: Fe_2O_3 is an active component in various widely used catalytic systems including the industrial process of conversion of styrene from ethylbenzene[40] and in new catalysts.[5,41] Fe-containing Pt alloy nanoparticles are one of the most promising materials for next generation ultrahigh density magnetic storage media applications, $L1_o$ phase FePt alloy in particular.[7]

Herein, we describe the synthesis and characterization of well-defined $Pt@Fe_2O_3$ nanoparticles using a sequential synthetic method. In a typical procedure, a mixture of 1,2-hexadecanediol (90%, tech. grade, Aldrich, 0.2 g or 0.75 mmol), oleic acid (99+%, Aldrich, 40 μL or 0.125 mmol), and oleylamine (70%, tech. grade, Aldrich, 40 μL or 0.125 mmol) in octyl ether (99%, Aldrich, 1.5 mL) was added into a 15 mL three-neck round-bottom flask under argon flow and heated to reflux temperature at 290 °C using a heating mantle. Platinum acetylacetonate ($Pt(acac)_2$) (99.99%, Aldrich, 0.1 g or 0.25 mmol) in octyl ether (1 mL) was injected into the mixture at this temperature. The color of the reaction solution turned black immediately, indicating the spontaneous formation of nanoparticles. The reaction continued for additional 5 min, and the solution was then cooled to 220 °C. A designed amount of iron pentacarbonyl ($Fe(CO)_5$) (99.999%, Aldrich) was added using a microsyringe, and the temperature of the reaction was raised to 290 °C. The solution refluxed at this temperature for a designed period of time (∼5 min to ∼2 h) and was then cooled to ambient room temperatures. After the reaction, the nanoparticles were separated from the mixture by washing with hexane and ethanol, respectively, and centrifuged at 5000 rpm for ∼5 min in ambient conditions. This procedure was repeated twice. The final product was dispersed in hexane with a small amount of excess oleic acid.

The low-magnification transmission electron microscopy (TEM) images were recorded on a JEOL JEM 2000EX microscope at an accelerating voltage of 200 kV. The high-magnification TEM images and compositional analyses of single nanoparticles were obtained using a FEI CM20 analytical electron microscope (AEM) equipped with an EDAX energy dispersive unit. Powder X-ray diffraction (PXRD) spectra of nanoparticles were recorded on a Philips MPD diffractometer with a Cu Kα (1.5405 Å) X-ray source. X-ray photoemission spectroscopy (XPS) was recorded on a Surface Science Laboratories SSX-100 instrument equipped with a monochromatic Al anode X-ray gun.

Figure 1 shows representative bright-field TEM images of core−shell nanoparticles made using a $Pt(acac)_2/Fe(CO)_5$ mole ratio of 1:2. The nanoparticles are relatively monodisperse, and the contrast between the core and shell of the nanoparticles was easily distinguishable in TEM images. The dark cores have an average diameter of ∼10 nm and possess well-defined crystalline facets with the morphologies that have been seen for cubic phase colloidal platinum nanoparticles.[42] High magnification TEM images show that the average shell thickness of these nanoparticles is ∼3.5 nm (Figure 1b). Crystalline structures of the core−shell nanoparticles were analyzed using PXRD (Figure 2). The X-ray diffractions at 39.8°, 46.3°, 67.5°, and 81.3° 2θ can be assigned to (111), (200), (220), and (311) planes of cubic phase platinum (*Fm*3*m*), respectively. The strong diffraction from Pt is not surprising because of the heavy atom effect.[43] The diffraction patterns of nanoparticles were relatively broad, most likely due to the small sizes of the nanoparticles.

It is known that PXRD is not an ideal method to characterize certain crystalline forms of iron-containing

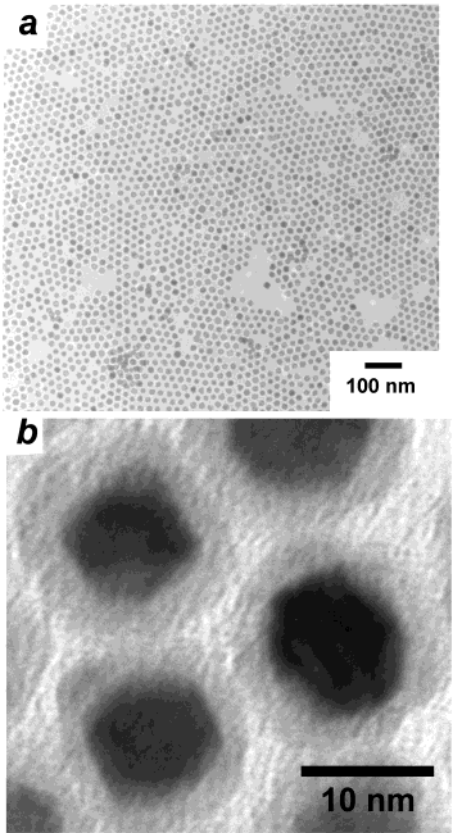

Figure 1. (a) Low and (b) high magnification TEM images of core−shell nanoparticles. The nanoparticles were made at the following reactant mole numbers in octyl ether (2.5 mL) for ∼15 min: $Pt(acac)_2$ (0.25 mmol), $Fe(CO)_5$ (0.5 mmol), 1, 2-hexadecanediol (0.75 mmol), oleic acid (0.125 mmol), and oleylamine (0.125 mmol).

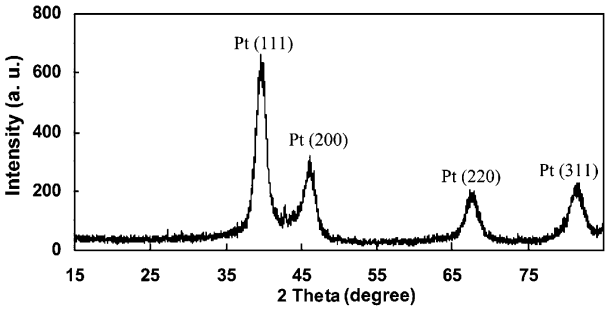

Figure 2. Representative PXRD spectrum of the core−shell nanoparticles.

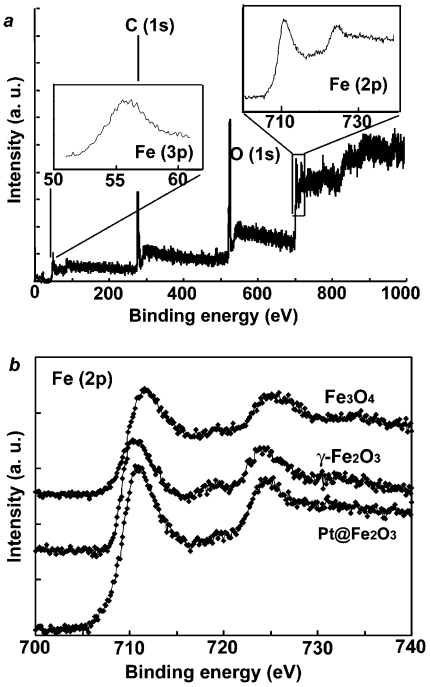

Figure 3. (a) XPS spectra of oleic acid stabilized Pt@Fe_2O_3 core−shell nanoparticles. Insets show expanded spectra of Fe 2p and 3p core lines; (b) XPS spectra of Fe 2p core-level lines for oleic acid stabilized Pt@Fe_2O_3 core−shell nanoparticles, γ-Fe_2O_3 and Fe_3O_4 powder references.

nanoparticles, such as γ-Fe_2O_3 (cubic maghemite) and Fe_3O_4 (magnetite), because they both possess the inverse spinel structure and can have similar PXRD patterns.[45] XPS was used to examine shell structure of these nanoparticles, because core electron lines of ferrous and ferric ions can both be detected and distinguishable in XPS. This technique has been used to differentiate between Fe_2O_3 and Fe_3O_4.[45−47] Figure 3a shows representative XPS spectra of the oleic acid stabilized core−shell nanoparticles. The photoelectron peaks at 710.9 and 724.9 eV are the characteristic doublet of Fe $2p_{3/2}$ and $2p_{1/2}$ core-level spectra of iron oxide, respectively (inset). A relatively weak Fe 3p line at 55.9 eV was also detected. Both Fe 2p and 3p data matched closely with those of Fe_2O_3 reported in the literature.[45] To further confirm the oxidation state of the iron oxide shells, we ran the references of Fe_3O_4 (98%, powder, < 5 micron, Aldrich) and γ-Fe_2O_3 (99.9%, Aldrich) powders under the same conditions as those for the core−shell nanoparticles (to rule out the discrepancy of XPS data due to the variation of instrumental conditions). Figure 3b shows the Fe 2p XPS spectra of both the two references and the core−shell nanoparticles. The binding energy of Fe $2p_{3/2}$ and $2p_{1/2}$ lines for these three different types of samples are summarized in Table 1. The XPS signals of the core−shell nanoparticles matched well with those of γ-Fe_2O_3 and differed from those of Fe_3O_4 by ∼1 eV. No metallic iron signals could be detected in the XPS spectra. The fact that no iron signal was observed suggested that Fe$(CO)_5$ decomposition was accompanied by the oxidation of iron either during the high-temperature reaction and/or the subsequent steps. The oxidation of surfactant stabilized iron-containing nanoparticles of metals and alloys has been

Table 1. Binding Energy (eV) of Core-Level Fe 2p Lines in Iron Oxides

sample	Fe_3O_4 powder[a]	γ-Fe_2O_3 powder[a]	core−shell nanoparticles
Fe $2p_{3/2}$	711.9	710.6	710.9
Fe $2p_{1/2}$	725.8	724.3	724.9

[a] Fe_3O_4 (98%, powder, < 5 micron) and γ-Fe_2O_3 (99.9%) reference solids were purchased from Sigma-Aldrich and used directly.

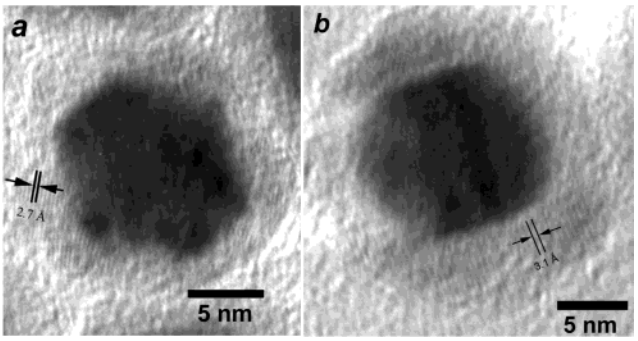

Figure 4. High-resolution TEM images of Pt@Fe_2O_3 nanoparticles showing the fringes of (a) (221) and (b) (220) crystal planes of γ-Fe_2O_3 shells.

previously reported.[31,38,44] Our convergent evidences from XPS, TEM and PXRD indicate that platinum is most likely not present in the shell layer since the detectable X-ray photoemission comes from the atoms in layers beneath the examined surfaces with a depth of ∼3−5 nm. The observed core-level XPS spectra of C 1s (287 eV) and O 1s (531 eV) come from oleic acid and iron oxide.

The fine structures of the shell layers were further characterized using high-resolution TEM. Figure 4 shows two representative TEM images that focus the crystalline structures of the shells of the nanoparticles. The shell layers, thin enough to be studied directly by TEM, typically had the same types of fringes running directly from the platinum crystalline surfaces. The fringes shown in Figure 4 have a spacing of ∼2.7 Å (Figure 4a) and ∼3.1 Å (Figure 4b), which match most closely to (221) and (220) planes of γ-Fe_2O_3 (cubic maghemite, $P4_232$), respectively. We were not able to obtain TEM images that show atomic lattices of the platinum cores, presumably due to the relatively large size of cores and the interference from the γ-Fe_2O_3 shells.

A distinct difference between the approach presented in this paper and those used in making metal alloys and other approaches of making nonalloy metal-containing nanoparticles in octyl ether[8,32] is that the presented method is used for making core−shell nanoparticles via a one-pot stepwise process. In this procedure, platinum precursors first reacted at the reflux temperature to form metal cores, which is followed by the addition of iron pentacarbonyl at a designed concentration in the same reaction vessel. This two-step route allows the shell thickness of the core−shell nanoparticles to be manipulated in a controlled manner. The ease of thermodecomposition of Fe$(CO)_5$ in hot organic solvents offers an additional advantage of making iron-containing species on preformed platinum nanoparticles in situ. Figure 5 shows

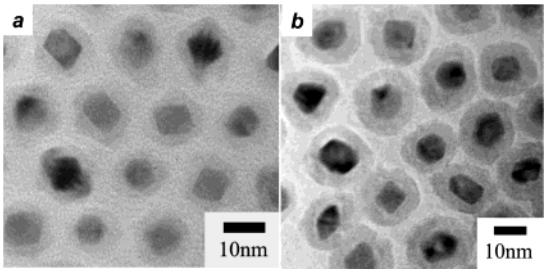

Figure 5. TEM images of Pt@Fe_2O_3 core−shell nanoparticles made at two different $Fe(CO)_5$ concentrations. The reactions last for ∼1 h at 290 °C. The nanoparticles were made at the following reactant mole numbers in octyl ether (2.5 mL): $Pt(acac)_2$ (0.25 mmol), $Fe(CO)_5$) (*n* mmol), 1,2-hexadecanediol (0.75 mmol), oleic acid (0.125 mmol), and oleylamine (0.125 mmol), where $n = 0.5$ (a) and 1.0 (b).

two TEM images of Pt@Fe_2O_3 core−shell nanoparticles obtained by injecting different amounts of $Fe(CO)_5$ into the reaction flasks immediately after Pt nanoparticles (∼10 nm) were formed. The nanoparticles shown in Figure 5a have an average shell thickness of ∼3.5 nm and were made with an $Fe(CO)_5$ final concentration of 0.2 mM. Increasing the final concentration of $Fe(CO)_5$ to 0.4 mM led to the thickening of Fe_2O_3 shells of the nanoparticles to ∼5.4 nm (Figure 5b).

In summary, we have shown that relatively monodisperse Pt@Fe_2O_3 core−shell nanoparticles can be synthesized using a one-pot sequential synthetic method. The thickness of the shells can be easily controlled by varying the initial concentrations of the reactants. The method presented in this paper could be used in making other transition-metal-containing core−shell nanoparticles. Pt@Fe_2O_3 core−shell nanoparticles could also find applications in catalysis and as precursor materials for making magnetically active nanocomposites for ultrahigh data storage media applications.

Acknowledgment. This work was supported by the University of Rochester and the U.S. Department of Energy (DOE) Office of Inertial Confinement Fusion under Cooperative Agreement No. DE-FC03-92SF19460. The support of the DOE does not constitute an endorsement by the DOE of the views expressed in this article. We are grateful to the Eastman Kodak Company for the in-kind analytical support. We thank Dr. Henry Gysling (Eastman Kodak Company) for helpful discussion.

References

(1) Ozin, G. A. *Adv. Mater.* **1992**, *4*, 612−649.
(2) Caruso, F. *Adv. Mater.* **2001**, *13*, 11−22.
(3) *Metal Clusters in Chemistry: Nanomaterials and Solid-State Cluster Chemistry*; Braunstein, P., Oro, L. A., Raithby, P. R., Eds.; Wiley-VCH: Weinheim, 1999; Vol. 3.
(4) Murray, C. B.; Kagan, C. R.; Bawendi, M. G. *Annu. Rev. Mater. Sci.* **2000**, *30*, 545−610.
(5) Klabunde, K. J.; Mulukutla, R. S. In *Nanoscale Materials in Chemistry*; Klabunde, K. J., Ed.; John Wiley and Sons: 2001, pp 223−261.
(6) Somorjai, G. A.; Borodko, Y. G. *Catal. Lett.* **2001**, *76*, 1−5.
(7) Weller, D.; Doerner, M. F. *Annu. Rev. Mater. Sci.* **2000**, *30*, 611−644.
(8) Sun, S. H.; Murray, C. B.; Weller, D.; Folks, L.; Moser, A. *Science* **2000**, *287*, 1989−1992.
(9) Prinz, G. A. *Science* **1998**, *282*, 1660−1663.
(10) Ross, C. *Annu. Rev. Mater. Res.* **2001**, *31*, 203−235.
(11) Josephson, L.; Perez, J. M.; Weissleder, R. *Angew. Chem., Int. Ed. Engl.* **2001**, *40*, 3204−3206.
(12) Jordan, A.; Scholz, R.; Maier-Hauff, K.; Johannsen, M.; Wust, P.; Nadobny, K.; Schirra, H.; Schimdt, H.; Deger, S.; Loening, S.; Lanksch, W.; Felix, R. *J. Magn. Magn. Mater.* **2001**, *225*, 118−126.
(13) Bulte, J. W. M.; Douglas, T.; Witwer, B.; Zhang, S. C.; Strable, E.; Lewis, B. K.; Zywicke, H.; Miller, B.; van Gelderen, P.; Moskowitz, B. M.; Duncan, I. D.; Frank, J. A. *Nature Biotechnol.* **2001**, *19*, 1141−1147.
(14) Zhong, C. J.; Maye, M. M. *Adv. Mater.* **2001**, *13*, 1507−1511.
(15) Schmid, G. In *Metal Clusters in Chemistry*; Braunstein, P., Oro, L. A., Raithby, P. R., Eds.; Wiley-VCH: Weinheim, 1999; Vol. 3, pp 1325−1341.
(16) Decker, S.; Klabunde, K. J. *J. Am. Chem. Soc.* **1996**, *118*, 12465−12466.
(17) Jiang, Y.; Decker, S.; Mohs, C.; Klabunde, K. J. *J. Catal.* **1998**, *180*, 24−35.
(18) Carnes, C. L.; Klabunde, K. J. *Chem. Mater.* **2002**, *14*, 1806−1811.
(19) Luo, J.; Maye, M. M.; Lou, Y.; Han, L.; Hepel, M.; Zhong, C. J. *Catal. Today* **2002**, *77*, 127−138.
(20) Khan, N. A.; Hwu, H. H.; Chen, J. G. *J. Catal.* **2002**, *205*, 259−265.
(21) *MRS Bull.* **1989**, *14*, 18−46.
(22) *MRS Bull.* **1990**, *15*, 16−47.
(23) LizMarzan, L. M.; Giersig, M.; Mulvaney, P. *Langmuir* **1996**, *12*, 4329−4335.
(24) Alejandro-Arellano, M.; Ung, T.; Blanco, A.; Mulvaney, P.; Liz-Marzan, L. M. *Pure Appl. Chem.* **2000**, *72*, 257−267.
(25) Lu, Y.; Yin, Y.; Li, Z.-Y.; Xia, Y. *Nano Lett.* **2002**, *2*, 785−788.
(26) Lu, Y.; Yin, Y.; Mayers, B. T.; Xia, Y. *Nano Lett.* **2002**, *2*, 183−186.
(27) Mayya, K. S.; Gittins, D. I.; Caruso, F. *Chem. Mater.* **2001**, *13*, 3833−3836.
(28) O'Connor, C. J.; Sims, J. A.; Kumbhar, A.; Kolesnichenko, V. L.; Zhou, W. L.; Wiemann, J. A. *J. Magn. Magn. Mater.* **2001**, *226*, 1915−1917.
(29) Park, J. I.; Cheon, J. *J. Am. Chem. Soc.* **2001**, *123*, 5743−5746.
(30) Portales, H.; Saviot, L.; Duval, E.; Gaudry, M.; Cottancin, E.; Pellarin, M.; Lerme, J.; Broyer, M. *Phys. Rev. B* **2002**, *65*, art. no.-165422.
(31) Ravel, B.; Carpenter, E. E.; Harris, V. G. *J. Appl. Phys.* **2002**, *91*, 8195−8197.
(32) Sobal, N. S.; Hilgendorff, M.; Mohwald, H.; Giersig, M.; Spasova, M.; Radetic, T.; Farle, M. *Nano Lett.* **2002**, *2*, 621−624.
(33) Sun, X.-C.; Nava, N. *Nano Lett.* **2002**, *7*, 765−769.
(34) Freeman, R. G.; Hommer, M. B.; Grabar, K. C.; Jackson, M. A.; Natan, M. J. *J. Phys. Chem.* **1996**, *100*, 718−724.
(35) Shibata, T.; Bunker, B. A.; Zhang, Z. Y.; Meisel, D.; Vardeman, C. F.; Gezelter, J. D. *J. Am. Chem. Soc.* **2002**, *124*, 11989−11996.
(36) Peng, X. G.; Schlamp, M. C.; Kadavanich, A. V.; Alivisatos, A. P. *J. Am. Chem. Soc.* **1997**, *119*, 7019−7029.
(37) Dabbousi, B. O.; Rodriguez-Viejo, J.; Mikulec, F. V.; Heine, J. R.; Mattoussi, H.; Ober, R.; Jensen, K. F.; Bawendi, M. G. *J. Phys. Chem. B* **1997**, *101*, 9463−9475.
(38) Sun, S. H.; Anders, S.; Hamann, H. F.; Thiele, J. U.; Baglin, J. E. E.; Thomson, T.; Fullerton, E. E.; Murray, C. B.; Terris, B. D. *J. Am. Chem. Soc.* **2002**, *124*, 2884−2885.
(39) Fievet, F.; Lagier, J. P.; Figlarz, M. *MRS Bull.* **1989**, *14*, 29−34.
(40) Elvers, B.; Hawkins, S.; Russey, W. In *Ullman's Encyclopedia of Industrial Chemistry*; 5th ed; VCH: Weinheim, 1994; Vol. A25, pp 329−339.
(41) Guczi, L.; Horvath, D.; Paszti, Z.; Peto, G. *Catal. Today* **2002**, *72*, 101−105.
(42) Ahmadi, T. S.; Wang, Z. L.; Green, T. C.; Henglein, A.; El-Sayed, M. A. *Science* **1996**, *272*, 1924−1926.
(43) Ladd, M. F.; Palmer, R. A. *Structure Determination by X-Ray-Crystallography*; Kluwer: Dordrecht, 1994.
(44) Fertman, V. E. *Magnetic Fluids Guidebook: Properties and Applications*; Hemisphere Publishing Corporation: New York, 1990.
(45) Cornell, R. M.; Schwertmann, U. *The Iron Oxides: Structure, Properties, Reactions, Occurrence and Uses*; VCH: Weinheim, 1996.
(46) McIntyre, N. S.; Zetaruk, D. G. *Anal. Chem.* **1977**, *49*, 1521−1529.
(47) Fujii, T.; de Groot, F. M. F.; Sawatzky, G. A.; Voogt, F. C.; Hibma, T.; Okada, K. *Phys. Rev. B* **1999**, *59*, 3195−3202.

NL025918Y